Heliyon 5 (2019) e02596

Contents lists available at ScienceDirect

Heliyon

journal homepage: www.heliyon.com

Heliyon

Research Article

Synthesis, DFT studies, molecular docking, antimicrobial screening and UV fluorescence studies on ct-DNA for novel Schiff bases of 2-(1-aminobenzyl) benzimidazole

Sugandha Singhal [a], Pankaj Khanna [b], Leena Khanna [a,*]

[a] University School of Basic and Applied Sciences, Guru Gobind Singh Indraprastha University, Sector 16-C, Dwarka, New Delhi, 110078, India
[b] Department of Chemistry, Acharya Narendra Dev College, University of Delhi, Kalkaji, New Delhi, 110019, India

ARTICLE INFO

Keywords:
Organic chemistry
Pharmaceutical chemistry
Pharmacokinetics
Antibacterial activity
Molecular docking
Schiff base ligands (SBs)

ABSTRACT

Novel Schiff bases (SBs) were synthesized by condensation of 2-(1-Amino benzyl) benzimidazole with heterocyclic and aromatic carbonyl compounds. The structural characterization was done using ^{1}H, ^{13}C NMR, FTIR and ES-MS spectroscopic techniques. The *in silico* pharmacokinetics showed that nearly all compounds obeyed Lipinski rule of 5 with low toxicity and metabolic stability. The global reactivity descriptors were calculated using DFT approach. The molecular docking result of SBs with ct-DNA suggested interaction *via* groove binding mode. The antibacterial activity was tested against *S. aureus* and *E. coli*, indicated significant inhibition than reference drug. The compound **4d** gave best results at 50 μg ml^{-1} concentrations. UV/Vis and Fluorescence spectroscopy tools were used to evaluate ct-DNA binding ability of compounds **4a–e** through hypochromic shift. The steady state fluorescence predicted a moderate binding constant of 1.12×10^{4} for **4d**, indicative of non-intercalative mode.

1. Introduction

The extensive use of conventional antibiotics has led to resistance in micro-organisms. *E. coli*, *S. aureus* and *K. pneumonia* show resistance towards fluoroquinolone, methicillin, carbapenem respectively [1, 2]. Antimicrobial resistance (AMR) is of great concern making antimicrobial treatment become ineffective and infections persist. Therefore, it has become crucial to develop new molecules acting as non-resistant antimicrobial agents. Also, small molecules targeting bacterial DNA are the most widely studied due to their better efficacy as drugs. However, their binding modes may vary from either minor groove binding or intercalation depending on selectivity towards specific DNA sequence [3, 4].

Many natural occurring alkaloids such as ellipticine, cryptolepine and synthetic derivatives of benzimidazoles i.e. Hoechst-33258, have been earmarked as important DNA intercalators [5]. Whereas indole and benzimidazole diamidine derivatives have been found to possess DNA groove binding ability along with antimicrobial action. There *in vitro* and *in vivo* actions were superior to the clinically approved DNA groove binding drug, pentamidine [6]. Thiabendazole, a well-known anthelmintic, was proved to be a minor-groove binder of ct-DNA [7].

However, researchers are always keen in designing new Mannich and Schiff base derivatives, as they are easy to prepare, possess great structural flexibility with DNA binding affinity. Schiff's Bases (SBs) of cinnamaldehyde, salicylaldehyde, 2-hydroxybenzaldehyde and 4-dimethylaminobenzaldehyde etc. have shown considerable antibacterial activity [8, 9, 10, 11]. The *in silico* and *in vitro* studies on indole based SBs have proved their antimicrobial potential [12, 13]. The SAR studies revealed that electron pair present on the nitrogen of the imine group is in sp^2 hybridized orbital and has been responsible for its DNA binding ability, leading to potential biological activities [14].

Owing to the above applicative importance of SBs and our constant endeavor to synthesize various biologically important heterocycles through SBs [15, 16, 17], we hereby report the synthesis of novel Schiff bases (SBs) as potential antimicrobial agents. One pot condensation reaction of heterocyclic amine with aryl/heteroaryl carbonyl compounds gave desired SBs. Benzimidazole was chosen as a heterocyclic amine due to its wide availability as a bioactive scaffold [2, 18] and diversified pharmaceutical applications [19, 20, 21, 22, 23, 24, 25, 26, 27, 28] with DNA minor groove binding capability [29].

Hence, novel Schiff Bases (SBs) have been prepared from the reaction of 2-(1-amino benzyl) benzimidazole with various aryl/heteroaryl carbonyl compounds. Further, computational studies including *in silico* DFT study to describe their chemical reactivity, toxicity screening (using PreAdmet Server) and molecular docking (using Autodock program 4.2)

* Corresponding author.
E-mail address: leenakhanna@ipu.ac.in (L. Khanna).

https://doi.org/10.1016/j.heliyon.2019.e02596
Received 30 April 2019; Received in revised form 27 June 2019; Accepted 1 October 2019

was performed. Antimicrobial screening and *in vitro* ct-DNA binding (using UV-Vis and Fluorescence Spectroscopy) ability and groove binding mode have been evaluated for the synthesized SBs.

2. Experimental

The melting points readings were taken using melting point apparatus in open capillary tube which are uncorrected. FTIR spectra were recorded on Bruker Tensor 37 FTIR spectrophotometer. The ^{13}C-NMR and ^{1}H-NMR spectra were recorded in $CDCl_3$ on Bruker Advance-II 400 NMR spectrometer with $CDCl_3$ as solvent. TMS was used as internal reference. Mass spectra were recorded at Waters, Q-TOF mass spectrometer at AIRF facility, JNU, New Delhi. The elemental analysis was recorded using EVO18 Zeiss SEM instrument at SAIIF, AIIMS, New Delhi. The compound purity was checked using commercialized (E-Merck Kieselgel 60 F254) silica plate. The chemicals were purchased from Merck and Alfa Aesar. General procedure for synthesis of 2-(1-amino benzyl) benzimidazole (**3a**): A mixture of *o*-phenylenediammine (0.012 mol) and phenylglycine (0.036 mol) in 40 ml 4N HCl was placed in a round-bottom flask. The reaction mixture was refluxed for 5 h and the progress of reaction was monitored *via* TLC. The pH of the reaction mixture after cooling was adjusted to 8 using solution of 1N sodium hydroxide. The obtained crude product was filtered and washed using water. The product was recrystallised using acetone. General procedure for the preparation of Schiff base derivatives **4** (**a–h**): To a suspension of 2-(1-amino benzyl) benzimidazole (**3a**) (0.02 mol) in 30 ml ethanol, an equimolar solution of corresponding aromatic/heterocyclic carbonyl compound was added. A few drops of glacial acetic acid were added to the mixture. The solution was stirred for 6 h at room temperature. The resultant precipitate was filtered, washed with ethanol followed by recrystallization.

2.1. Calculation of pharmacokinetic and toxicity parameters

The Molinspiration cheminformatics software (www.molinspiration.com) was used to calculate molecular properties of synthesized compounds **4a–h**. In order to evaluate drug likeliness parameters such as number of atoms, molecular weight, partition coefficient (Log P), topological surface area (TPSA), hydrogen bond donors and acceptors, and Lipinski's rule violations were calculated. Adsorption, distribution, metabolism and excretion (ADME) features were calculated using PreADMET online server version 2.0. The ADME parameters include plasma protein binding (PPB), human intestinal absorption (HIA), logKp (degree of skin permeation), Caco2 cell lines and MDCK cell lines to determine oral absorption.

2.2. In silico DFT calculation

The chemical reactivity and global reactivity descriptors for the synthesized SBs **4a–h** were calculated using DFT study at B3LYP/6-311G++(d,p) level of computation using Gaussian 09 software.

2.3. Molecular docking

AutoDock 4.2 along with Auto Dock Tools (Graphical Interface program) was used to perform docking simulation. The DNA structure was retrieved from Protein Data Bank (PDB ID: 1BNA). The receptor and ligand files were corrected using Discovery Studio Visualizer 2017. The heteroatoms were removed from 1BNA.pdb, to remove any free ligand from complex receptor. DNA was prepared by addition of Kollman united atom charges, polar hydrogen's and solvation parameters. Ligands were prepared by assignment of Gasteiger charge and merging of non-polar hydrogens. The grid dimensions were kept 60, 60, 60 Å in x, y, z directions respectively. The search for best conformers was done using Lamarckian Genetic Algorithm (LGA). A maximum of 10 conformers were considered for each compound. Discovery Studio Visualizer 2017 was used for the visualization of docked poses. The results include predicted free energy of binding and binding interactions.

2.4. Antimicrobial activity

The antibacterial action of compounds **4a–h** was tested against gram positive and gram negative bacteria, *E. coli* and *S. aureus* respectively, by disc diffusion method. The bacterial culture was obtained from IMT Chandigarh. The minimum inhibitory concentration (MIC) values were evaluated at two different concentrations 50 and 100 μg/ml in DMSO solvent. The discs saturated with prepared solutions of compounds were placed on Nutrient agar plates seeded with tested bacteria. These plates were kept for 24 h incubation at 37 °C and the inhibition zone measurements (mm) were done. Experiments were triplicated with DMSO as negative control [30, 31, 32, 33, 34]. The results were compared with Ciprofloxacin sample as a standard (positive control).

2.5. Electronic absorption titration study

The UV absorbance for the corresponding compounds was recorded *via* UH5300 Double beam Spectrophotometer using cuvette of 1 cm path length. The SBs solutions (100 μM) were prepared in methanol. The ct-DNA stock was prepared in Tris-HCl buffer solution. The ctDNA solution (5mg in 2ml tris buffer) was prepared to get concentration of 15μM. The absorption titration was performed in absence and presence of ct-DNA. The concentration of ct-DNA was varied while that of ligand kept constant and measurements were done at wavelength 200–500 nm.

2.6. Fluorescence titration study

Fluorescence measurements were recorded using Agilent Technologies Cary Eclipse Fluorescence Spectrophotometer model no. MY13340005 equipped with a 150W Xenon lamp using a 1.00 cm quartz cell. The scanning parameters were optimized for 10 nm slit width, for excitation and emission, 0.2 s dwell time and 0.5 nm wavelength step. Fluorescence measurements parameters included excitation wavelength 290 nm, room temperature and wavelength scan range of 300–550 nm. The fluorescence titration was performed with a constant SB concentration (100 μM) and varying the ct-DNA concentration from 0-15 μM.

3. Results and discussion

3.1. Chemistry

A series of aryl/heteroaryl carbonyl compounds was selected to design and synthesize a set of SBs **4a–h** from heterocyclic amine (**3a**) [28]. The synthetic scheme for the target SBs and their corresponding structures have been given in Scheme 1. 2-(1-Amino benzyl) benzimidazole (**3a**) was prepared by refluxing *o*-phenylenediamine and phenylglycine for 5 h. The SBs were prepared by reaction of various aryl/heteroaryl carbonyl compounds with 2-(1-amino benzyl) benzimidazole. The structural determination of the synthesized compounds (**3a, 4a–4h**) was performed using ^{1}HNMR, ^{13}CNMR, FTIR and ES-MS spectroscopy techniques. The FTIR spectrum of compound **3a** depicted $-NH_2$ stretching vibrations (3352 cm^{-1}), –NH stretching frequency (3305 cm^{-1}), CH stretch of aromatic ring (3052 cm^{-1}), aliphatic CH stretch (2889-2661 cm^{-1}), aromatic C=C stretch (1652 cm^{-1}), C–N stretch (1155 cm^{-1}). In the ^{1}H NMR spectrum, the aliphatic C–H proton peak resonance observed as triplet at δ 4.32 ppm. The $-NH_2$ protons peak recorded as doublet at δ 2.03 ppm while the –NH peak of the benzimidazole resonated at 2.45 ppm. The aromatic protons recorded between δ 7.26–7.37 ppm. While in ^{13}C NMR spectrum, the methine carbon peak observed at 55.8 ppm while signal due to aromatic carbons appeared in the range δ 115.4–132.5 ppm. The ES-MS analysis results were in well agreement with the calculated mass of the compounds.

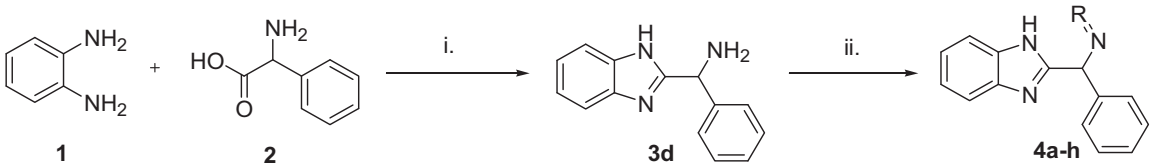

i. HCl, Reflux, 5 h; ii. Aryl/heteroaryl carbonyl compounds, rt, 6 h, C_2H_5OH; R=aryl/heteroaryl

Series1	a	b	C	D	e	F	g	h
R	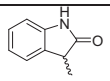	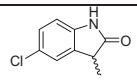	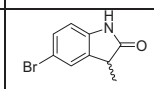	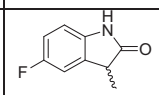	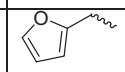			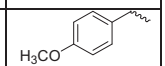
Yield	86%	84%	83%	83%	75%	76%	78%	79%

Scheme 1. Synthetic protocol for 2-(1-Amino benzyl) benzimidazole Schiff base derivatives **4a–4h**.

The spectroscopic analysis of representative SB, **4d** showed various stretching frequencies in FTIR spectrum, NH (3740 cm^{-1}), aliphatic CH (2884-2656 cm^{-1}), C=O of indole moiety (1752 cm^{-1}), C=N of azomethine group (1655 cm^{-1}), aromatic C=Cs (1577 cm^{-1}), C–N (1149 cm^{-1}) and C–F stretch (1016 cm^{-1}). In the ^{1}H NMR spectrum the aliphatic –CH peak obtained as singlet at δ 4.25 ppm. The occurrence of azomethine (C=N) stretch in FTIR spectrum and the CH peak shift from the parent compound **3** in ^{1}H NMR spectrum validated the formation of SB **4d**. The NH peak of benzimidazole resonated at 8.18 ppm while aromatic protons peak observed between δ 6.76–6.84 ppm. In the ^{13}C NMR spectrum, the methine carbon resonated at δ 55.8 ppm while a characteristic carbonyl carbon of indole signals at δ 161.2 in addition to a signal at δ 141.7, confirming the presence of azomethine (C=N) in the molecule. The signals due to aromatic carbons appeared in the range δ 115.2–132.5 ppm. Also, Elemental analysis and ES-MS results were same as the calculated molecular mass value. Similarly, detailed spectral analysis for other compounds **4a–4h** is provided in Table 1.

The synthesized SBs **4a–h** were screened *via in silico* calculations, i.e. pharmacokinetic parameters including ADME, DFT (frontier orbital calculations) and molecular docking study. Further, they were subjected to *in vitro* antibacterial action, which filtered out few lead compounds for DNA binding study. The DNA binding was assessed using UV-Vis and Fluorescence spectroscopy to support molecular docking assessment.

3.2. Pharmacokinetic and ADME parameters

All the compounds fitted well *via* Lipinski's rule of five (MW < 500, Log P < 5, number of H bond donors up to 5 and H bond acceptors up to 10)

Table 1
Spectral Data of synthesized compound 3a and SBs **4a–h**.

Comp.	M.P. (°C)	IR (cm^{-1})	EIMS, m/z	^{1}H NMR 400MHz (δ, $CDCl_3$)	^{13}C NMR 75.5 MHz (δ, $CDCl_3$)	Elemental Analysis
3a	280	3352 (NH_2), 3305 (N–H), 3052 (Ar C–H), 2889, 2661 (CH_3C–H), 1155 (C–N), 1592 (Ar C=C)	224 $(M+H)^+$	2.03 (2H,d,NH_2), 2.45 (1H,s,NH), 4.32 (1H,s,CH), 7.26–7.37 (9H,m,Ar–H)	55.8, 115.4–132.5 (Ar carbons)	Calcd.: C, 75.31; H, 5.87; N, 18.82; found: C, 75.34; H, 5.85; N, 18.81
4a	312	3305 (N–H), 3052 (Ar C–H), 2889, 2661 (-CH), 1652 (C=N), 1155 (C–N), 1577 (Ar C=C)	352.38 (M^+)	8.18 (2H,s,NH), 4.25 (1H,s,CH), 6.65–6.77(4H,m,Ar–H), 6.83–6.85 (9H,m,Ar–H)	55.8, 115.2–141.5 (Ar carbons), 122.1–169.3 (Ar carbons- indole)	Calcd.: C, 74.98; H, 4.58; N, 15.90; found: C, 74.95; H, 4.59; N, 15.92
4b	315	3740 (N–H), 2882, 2665 (C–H), 1742 (C=O), 1575 (Ar C=C), 1149 (C–N), 1652 (C=N), 1155 (C–N), 727 (C–Cl)	386.83 (M^+)	8.18 (2H,s,NH), 4.25 (1H,s,CH), 6.65–6.77(4H,m,Ar–H), 6.83–6.85 (9H,m,Ar–H)	55.8, 115.2–141.5 (Ar carbons), 121.7–164.3 (Ar carbons- indole)	Calcd.: C, 68.31; H, 3.9; N, 14.48; Cl, 9.16; found: C, 68.33; H, 3.9; N, 14.46; Cl, 9.15
4c	318	3702 (N–H), 2882, 2655 (C–H), 1745 (C=O), 1577 (Ar C=C), 1652 (C=N), 1148 (C–N), 682 (C–Br)	431.28 (M^+)	8.18 (2H,s,NH), 4.27 (1H,s,CH), 6.78–6.85 (3H,q,Ar–H), 7.24–7.25 (9H,m,Ar–H)	55.8, 115.2–141.5 (Ar carbons), 122.2–164.3 (Ar carbons-indole);	Calcd.: C, 61.27; H, 3.51; N, 12.99; Br, 18.53; found: C, 61.28; H, 3.52; N, 12.97; Br, 18.55
4d	312	3740 (N–H), 2882, 2665 (C–H), 1742 (C=O), 1577 (Ar C=C), 1652 (C=N), 1149 (C–N)	370.28 (M^+)	8.18 (2H,s,NH), 4.25 (1H,s,CH), 6.65–6.77 (4H,m,Ar–H), 6.83–6.85 (9H,m,Ar–H)	55.8, 115.2–141.7 (Ar carbons), 122.1–169.3 (Ar carbons-indole)	Calcd.: C, 71.34; H, 4.08; N, 15.13; F, 5.13; found: C, 71.35; H, 4.06; N, 15.15; F, 5.12
4e	296	3305 (N–H), 2881, 2655 (C–H), 1700 (C–O), 1577 (Ar C=C), 1652 (C=N), 1148 (C–N)	301.34 (M^+)	4.11 (1H,s,CH), 4.28 (1H,s,CH), 6.65 (2H,dd, Ar–H), 6.75–6.78 (4H,q,Ar–H), 6.81–6.84 (5H,m,Ar–H), 7.26 (1H,t,Ar–H), 8.18 (1H,s,NH)	55.8, 110.3–164.2(Ar carbons)	Calcd.: C, 75.37; H, 5.02; N, 13.94; found: C, 75.38; H, 5.05; N, 13.90
4f	290	3462 (N–H), 2882, 2655 (C–H), 1577 (Ar C=C), 1652 (C=N), C–N (1149)	311.37 (M^+)	4.11 (1H,s,CH), 4.28 (1H,s,CH), 6.77–6.84 (4H,m,Ar–H), 7.24–7.26 (10H,m,Ar–H), 8.18 (1H,s,NH)	55.8, 122.4.-164.3(Ar carbons)	Calcd.: C, 81.00; H, 5.50; N, 13.49; found: 81.03; H, 5.48; N, 13.48
4g	294	3305 (N–H), 2881, 2655 (C–H), 1576 (Ar C=C), 1652 (C=N), 1148 (C–N)	361.43 (M^+)	4.11 (1H,s,CH), 4.28 (1H,s,CH), 6.76–6.84 (7H,m,Ar–H), 7.25–7.26 (9H,m,Ar–H), 8.18 (1H,s,NH)	55.8, 122.4–169.3(Ar carbons)	Calcd.: C, 83.08; H, 5.30; N, 11.63; found: C, 83.09; H, 5.33; N, 11.59
4h	298	3305 (N–H), 2881, 2655 (C–H), 1577 (Ar C=C), 1652 (C=N), 1148 (C–N)	341.40 (M^+);	4.05 (3H,s,OCH_3), 4.05 (1H,s,CH), 4.279 (1H,s,CH), 6.77–6.84 (4H,q,Ar–H), 7.2–7.26 (9H,m,Ar–H), 8.18 (1H,s,NH)	55.8, 60.2, 122.4–164.2(Ar carbons)	Calcd.: C, 77.40; H, 5.61; N, 12.31; found: C, 77.38; H, 5.63; N, 12.30

Table 2
Drug likeliness properties of synthesized SBs **4a–4h**.

Property	Compounds								
	3a	**4a**	**4b**	**4c**	**4d**	**4e**	**4f**	**4g**	**4h**
Log P	2.5	4.32	4.97	5.0	3.48	3.80	4.55	5.71	4.58
TPSA	54.71	73.91	73.91	73.91	73.91	54.19	41.05	41.05	50.28
Natoms	17	27	28	28	28	23	24	28	26
MW	223.28	352.4	386.84	431.29	370.39	301.35	311.39	361.45	341.41
nOH	3	5	5	5	5	4	3	3	4
nOHNH	3	2	2	2	2	1	1	1	1
Nviolations	0	0	0	0	0	0	0	1	0
Nrotb	2	3	3	3	3	4	4	4	5
Volume	208.39	312.31	325.85	330.20	317.25	273.34	291.77	335.76	317.32

Table 3
ADME Properties of synthesized SBs **4a–h**.

Property	Compounds								
	3a	**4a**	**4b**	**4c**	**4d**	**4e**	**4f**	**4g**	**4h**
BBB	2.19	2.32	2.87	3.03	2.10	4.78	9.01	11.18	6.83
Caco 2	19.23	24.84	29.76	29.46	34.77	24.29	27.51	27.93	56.64
HIA	90.53	92.68	93.42	93.80	92.70	93.70	94.16	94.75	92.72
MDCK	354.59	221.71	112.82	4.30	181.03	59.88	100.48	77.09	112.82
PPB*	46.34	87	89	88	89	90	92	89	87
SP*	-3.87	-3.99	-4.09	-3.94	-4.33	-2.48	-2.42	-2.14	-3.12

*BBB: Blood Brain Barrier. *HIA: Human Intestinal Absorption. *PPB: Plasma Protein Binding. *SP: Skin Permeability.

except **4g** with one violation (Table 2). The ADME parameters given in Table 3 predicted good pharmacokinetics and bioavailability. The HIA values were above 90% indicated good oral absorption of the compounds. The negative Kp values indicated poor skin permeability resulting in good oral absorption. In case of accidental contact to skin no effect will be observed. The PPB values were less than 90% except **4g**. The Caco 2 values were in between 4-70 considered moderately permeable. The MDCK values greater than 25 showed good absorption for compounds except **4c**. However, other parameters need to be taken into account.

3.3. Fronteir orbital calculation

The HOMO (highest occupied molecular orbital) and LUMO (lowest unoccupied molecular orbital) frontier orbitals signify chemical reactivity and active sites of compounds. The negative chemical potential indicates non-spontaneous decomposition. The values of HOMO, LUMO energies and global reactivity descriptors are summarized in Table 4. The HOMO, LUMO plots for the parent precursor **3a** and SB **4f** is depicted in Fig. 1. The low energy gap value signifies high chemical reactivity. The global reactivity descriptors such as chemical potential (μ), hardness (η), were calculated using Koopman's theorem equations:

The hardness is given by $\eta = \frac{I-A}{2}$

The chemical potential is given by $\mu = -(I+A)/2$

Table 4
Electronic energy calculation values of synthesized SBs **4a–h**.

Compound	E_{HOMO}	E_{LUMO}	Energy gap	μ	η	χ
3a	-0.3334	-0.1744	0.1590	-0.2539	0.0795	0.2539
4a	-0.0641	-0.0075	0.0566	-0.0358	0.0283	0.0358
4b	-0.0713	-0.0152	0.0561	-0.0432	0.0280	0.0432
4c	-0.0675	-0.0113	0.0562	-0.0394	0.0281	0.0394
4d	-0.0639	-0.0077	0.0562	-0.0358	0.0281	0.0358
4e	-0.1654	-0.0373	0.1281	-0.1013	0.0640	0.1013
4f	-0.3187	-0.1959	0.1228	-0.2573	0.0614	0.2573
4g	-0.3186	-0.1964	0.1222	-0.2575	0.0611	0.2575
4h	-0.2221	-0.0458	0.1763	-0.1339	0.0881	0.1339

*μ is the chemical potential which indicates spontaneous decomposition. *η is the hardness. *χ is the electronegativity.

The electronegativity is given by $\chi = (I+A)/2$ Where I is electron affinity ($I = -E_{HOMO}$) and A is ionization potential ($A = -E_{LUMO}$).

The SBs **4a–d** had lower energy gap values within range 0.0561–0.0566 than the parent precursor **3a** with value of 0.1590. The SBs **4e–h** had values in the range 0.1222–0.1763. The energy gap values for the heteroaromatic derivatives were lower than counter aromatic ones.

3.4. Molecular docking

The molecular docking technique helps in understanding non-covalent drug-DNA interactions of small molecules into the targeted region of DNA for rational drug design and discovery. The minor groove of DNA is preferred over major one due to lesser steric hindrance, electrostatic factors and its narrow shape [35, 36, 37, 38, 39, 40].

The free energy binding values for the synthesized compounds **4a–e** were in the range -8.47 to -7.36 kcal/mol. The low binding scores for compounds **4f–h** indicated weak binding of the respective derivatives (Table 5). The interaction energies for top 5 best conformer poses of compound **4d** with ct-DNA have been evalulated and shown in Fig. 2 and Fig. 3. The energetically filtered best poses for compounds **4a–e** are shown in Fig. 4. The best poses for derivatives, **4f–h** are given in Fig. 5. The results clearly claimed strong and spontaneous groove binding of SBs rather than intercalation mode. The non-covalent interactions include H-bond, pi-pi stacking, pi-anion and pi-donor. The compound **4d** with highest binding energy was found to form H-bond with oxygen atom of residue adenine 17 *via* imidazole nitrogen (NH) atom at distance 2.15 Å. The pi-pi stacking interactions were observed between imidazole ring and adenine 17 and 18 residues; as well as between pyrrole ring of indole and guanine 16 and 17 residues. Pi-anion interaction between benzimidazole ring and oxygen atom of residue adenine 17, pi-donor between phenyl ring and nitrogen atom of residue adenine 18, were other important bindings observed.

Therefore, the *in silico* studies validate that SBs **4a–e** exhibited good binding affinity for target DNA and hence, can be further studied for their *in vitro* effect.

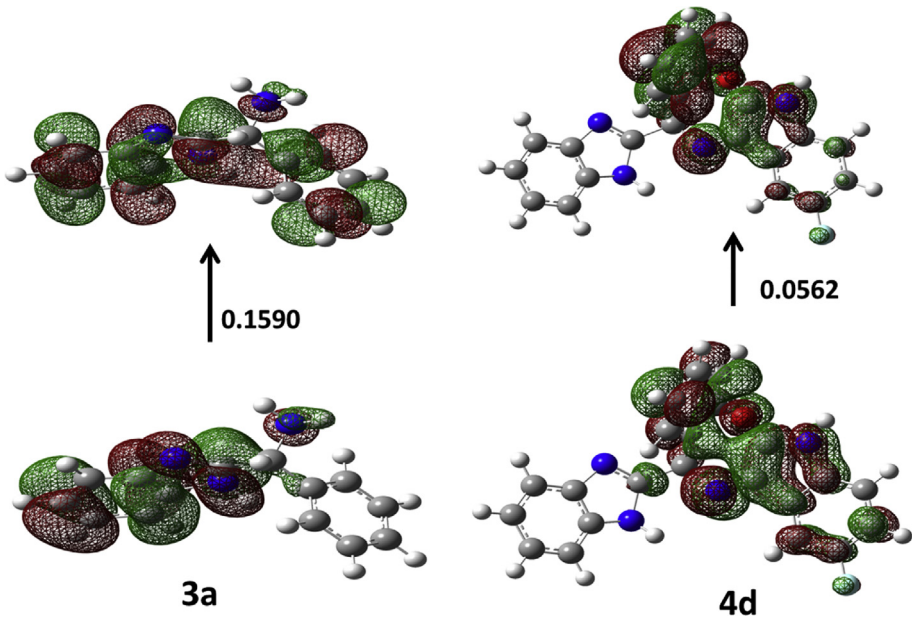

Fig. 1. HOMO-LUMO plots for 2-(1-amino benzyl) benzimidazole, **3a** and synthesized SB **4d**.

Table 5
Docking parameters via Autodock4.2

Compounds	Property		
	Free Energy of Binding Kcal/mol	Inhibition constant at 298.15 K (μM)	RMSD from reference structure
4a	-8.17	1.90	70.17
4b	-7.71	2.24	73.04
4c	-8.24	4.01	74.55
4d	-8.47	0.512	75.33
4e	-7.36	0.617	78.90
4f	-2.37	24.98	78.22
4g	-2.32	28.09	79.21
4h	-3.41	15.41	70.06

3.5. Antibacterial activity

The antibacterial activity of synthesized SBs (**4a–h**) against bacterial strains *E. coli* and *S. aureus* was evaluated. The three dimensional graphical representation and experimental details for zone of inhibition are given in Fig. 6 and Table 6. The results indicated that SB **4d** showed high activity against *E. coli*, even at MIC value 50 μg/ml, whereas lower activity was observed against *S. aureus*. The SBs **4b, 4c, and 4e** have moderate inhibition in *E. coli* and a reduced amount of activity in *S. aureus*. The rest of the SBs (**4a, 4f, 4g, and 4h**) gave lower activity in *E. coli* and *S. aureus*. The results signified that SBs obtained from heterocyclic carbonyl compounds had better antimicrobial action than the aromatic ones.

Hence, on the basis of *in silico* pharmacokinetics, ADME, Fronteir

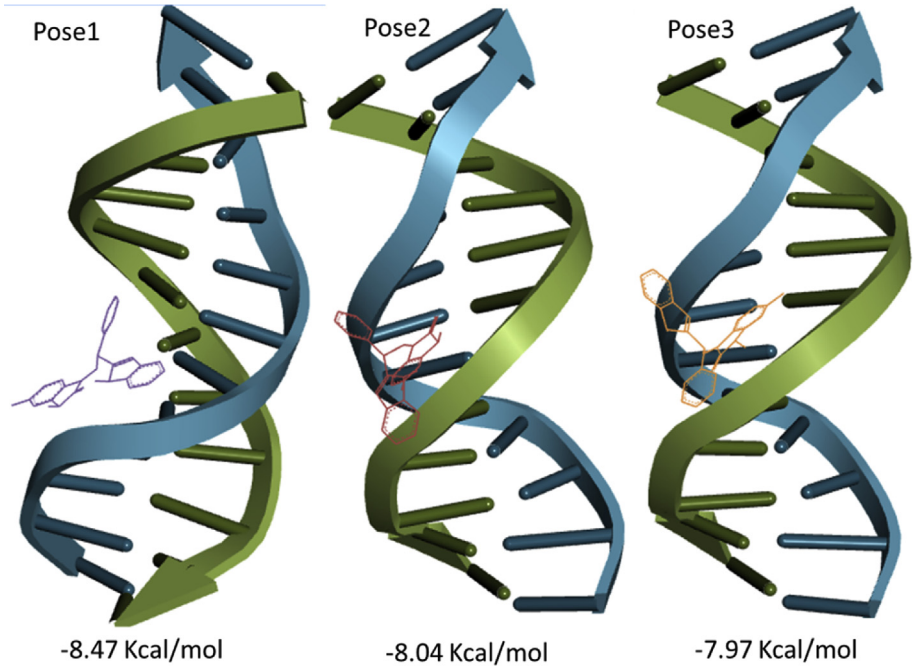

Fig. 2. Docked poses 1–3 of compound 4d within minor grove of ct-DNA (PDB ID: 1BNA).

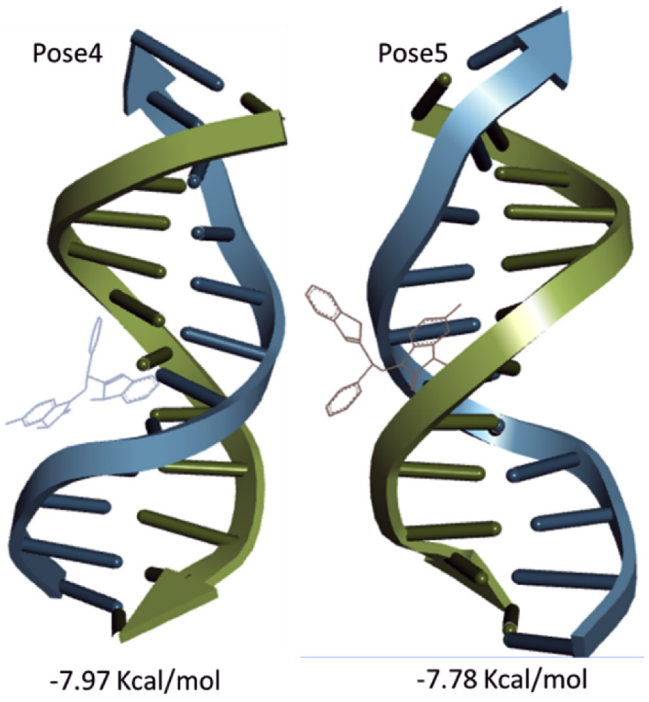

Fig. 3. Docked poses 4 and 5 of compound 4d within minor grove of ct-DNA (PDB ID: 1BNA).

orbital calculations, molecular docking and *in vitro* antibacterial results SBs **4a–e** were filtered to be more potent and lead compounds. Therefore, they were further screened for DNA binding activity *via* UV-Vis, Fluorescence spectroscopy.

3.6. UV visible spectroscopy

The UV-Vis spectrum for SBs **4a–e** gave peaks of high intensity at 250 nm and of low intensity at 390 nm, corresponding to $\pi \rightarrow \pi^*$ and $n \rightarrow \pi^*$transitions for azomethine group, respectively. Titration of SBs with aliquots of ct-DNA resulted in hyperchromism at 250 nm and hypochromism at 390 nm with no apparent wavelength shift. This hyperchromic effect resulted from conformational and structural changes of DNA upon interaction with compounds. The hypochromic effect resulted from DNA helix contraction. The binding of SBs clearly indicated isosbestic point at 340 nm indicated 1 mode of binding or balance of 1:1 receptor-drug stoichiometry (Fig. 7). Literature revealed that intercalating molecules display significantly large change in intensity and wavelength as compared to groove binders [7]. Therefore, UV titration results strengthen the proposed SBs groove binding ability with ct-DNA.

3.7. Fluorescence quenching studies

It is well known that the endogenous fluorescence property of DNA is poor; hence, the steady state fluorescence spectrum of SBs **4a–e** was investigated for the profound interactive binding study between them and DNA. The SBL **4d** and ct-DNA fluorescence titration emission spectrum is represented in Fig. 8a. **4d** gave two peaks at 344 and 353 nm when excited at 290 nm. The intensity of these observed peaks was decreased with subsequent ct-DNA addition, indicative of the complex formation and strengthening interaction between ct-DNA and SB **4d**.

As a result of certain molecular interactions such as molecular level rearrangement, excited state reactions, and ground complex formation among others, a decrease in fluorescence intensity is observed known as fluorescence quenching. Further, fluorescence quenching efficiency can be evaluated using Stern-Volmer quenching constant (Ksv) as per the Stern-Volmer equation.

$$\left(\frac{Fo}{F}\right) = 1 + Ksv\,[Q]$$

The parameters Fo and F depict the fluorescence intensities before and after the quencher addition while [Q] is the quencher concentration. The value of Ksv was obtained from the slope of plot (Fo/F) vs (ct-DNA) (Fig. 8b). The value was calculated to be 8.78×10^4 L mol^{-1} for **4d**, which was lower from reported value for intercalators and hence, emphasizing for non-intercalative mode of binding.

The linearity of Stern-Volmer plot typically described the nature of quenching process, dynamic or static which can further be differentiated from the following equation.

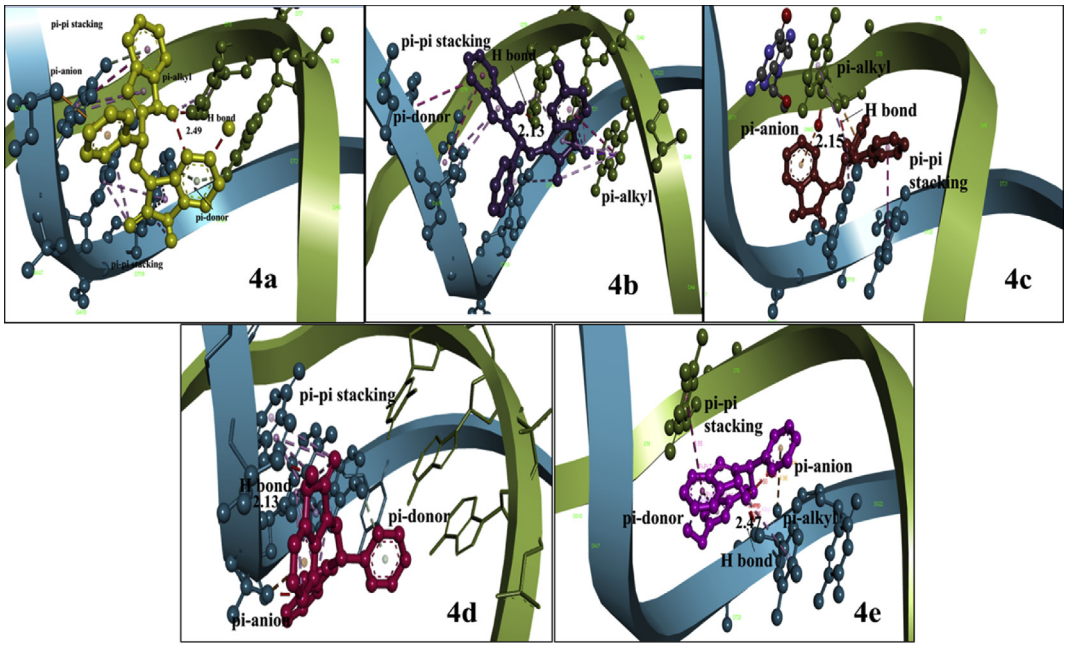

Fig. 4. Docking of compounds **4a–e** with ct-DNA (PDB ID: 1BNA).

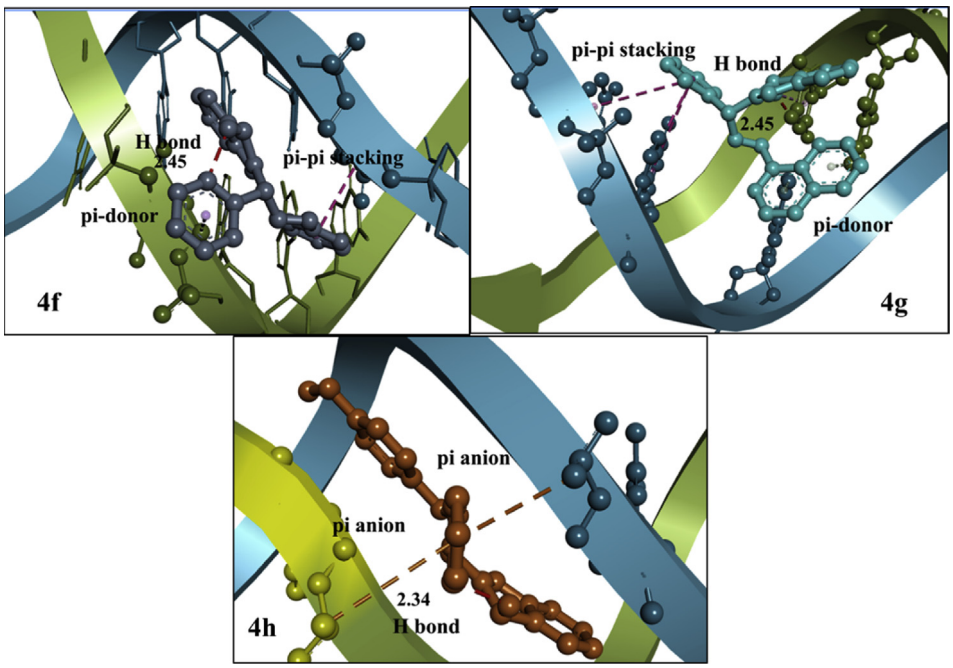

Fig. 5. Docking of compounds **4f–h** with ct-DNA (PDB ID: 1BNA).

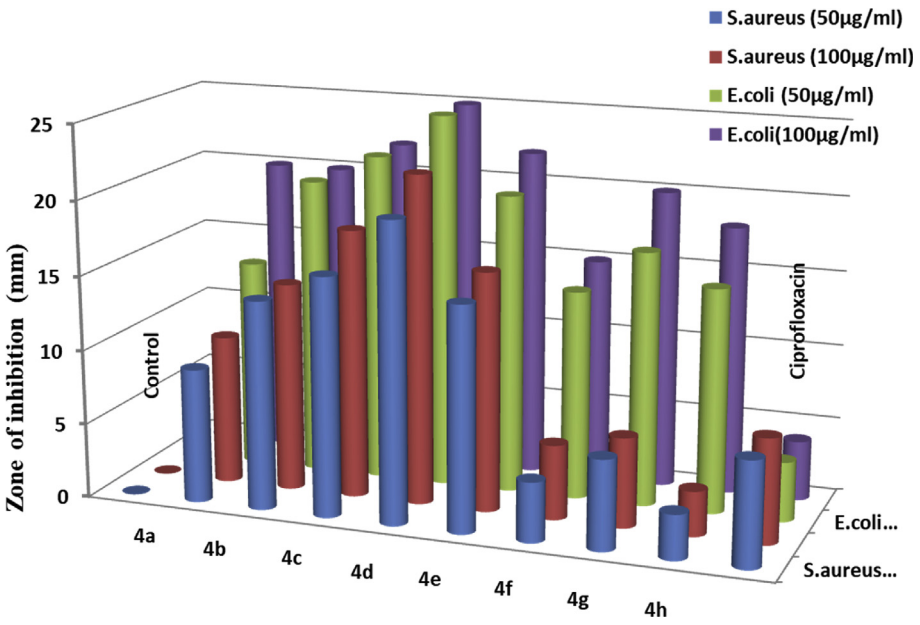

Fig. 6. Antibacterial activity of SBs (**4a–h**) against Gram positive and Gram negative bacteria (50 and 100 µg/ml concentration).

Table 6
Antimicrobial activity [zone of inhibition (mm)] of synthesized SBs (**4a–h**) against *E.coli* and *S.aureus*.

Compound Conc ug/ml	Control (DMSO) (+ve Control)	4a	4b	4c	4d	4e	4f	4g	4h	Reference (Ciprofloxin) (-ve Control)
E.coli 50ug/ml (inhibiton/mm)	0	14	20	22	25	20	14	27	25	14
E.coli 100 mg/ml (inhibiton/mm)	0	20	20	22	25	22	15	30	28	14
S.aureus 50ug/ml (inhibiton/mm)	0	9	14	16	20	15	14	16	13	17
S.aureus 100 mg/ml (inhibiton/mm)	0	10	14	18	22	16	15	16	13	17

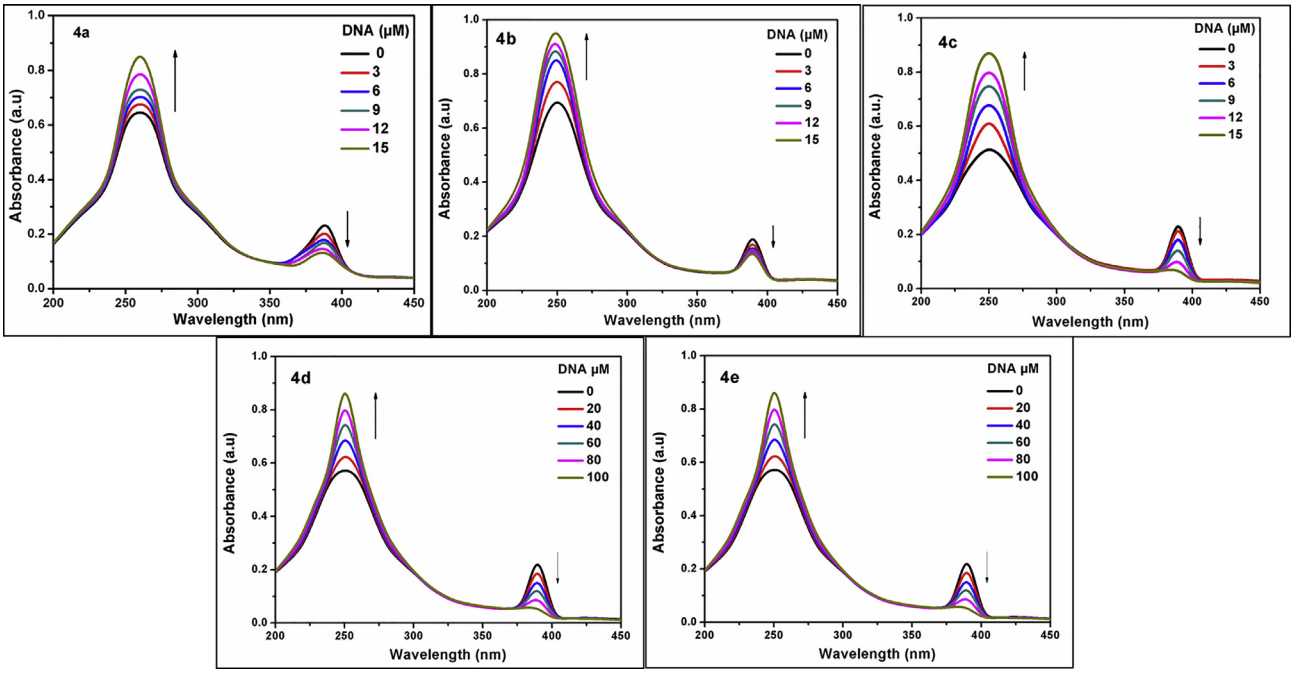

Fig. 7. UV-Vis interaction of SBs **4a**–**4e** (100 μM) with increasing concentration of ct-DNA.

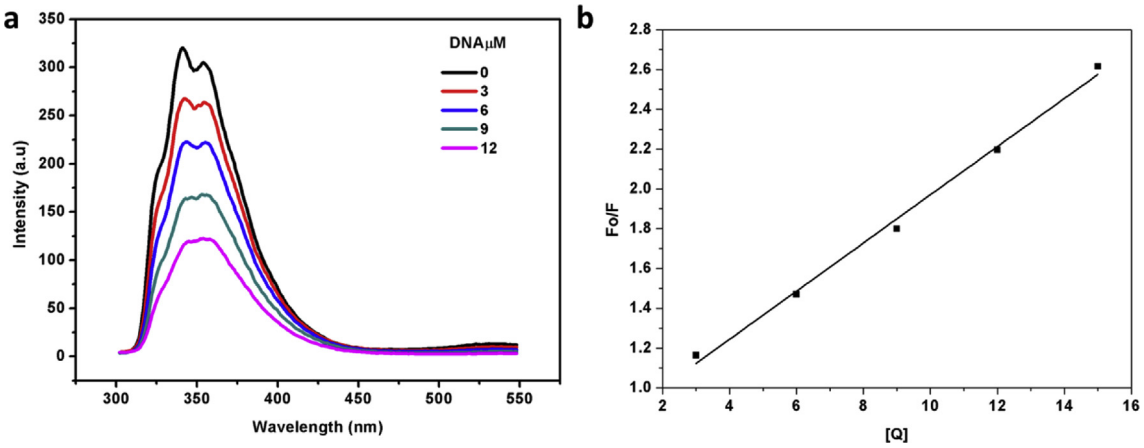

Fig. 8. Fluorescence of **4d** (a) titration quenching spectrum (b) Stern-Volmer quenching plot.

$$Kq = Ksv/\tau o$$

where Kq represents the apparent biomolecular quenching rate constant and τo, the fluorescence lifetime of the biomolecule in absence of quencher. The value for τo is 10^{-8} s. The value of Kq was calculated to be 8.78×10^{12} M^{-1} using the above equation. For biomolecules the limiting diffusion rate constant is around 2.0×10^{10} L mol^{-1} s^{-1}. If the calculated Kq value is higher than this value, the quenching process is static instead of dynamic. The higher Kq value as compared to reported limiting diffusion rate constant value signified complex formation quenching mechanism rather than dynamic collision.

3.8. Binding equilibrium

The binding constant (K) and the number of binding sites (n) can be calculated from the following equation.

$$log\frac{Fo-F}{F} = logK + n\log[Q]$$

The parameters Fo and F represent the fluorescence intensities for the fluorophore in the absence and presence of quencher. The values of K and n can be calculated using plot of log [(Fo-F)/F] vs. log [Q]. The plot obtained is linear whose slope equals to 'n' (the number of binding sites of SBs on ct-DNA) and the intercept equals logK (Fig. 9).

The values for K and n are given in Table 7. The binding constant for **4d** was calculated to be 1.12×10^4 M^{-1} at 293 K which is comparable to the value of 6.32×10^3 M^{-1} reported for thiabendazole [7]. The binding constant values for the SBs **4a–d** and a few reported groove binding drugs [41, 42, 43] are listed in Table 7. The low value of binding constant supported the grove binding mode rather than the intercalative mode into DNA. The n value of 1.1 indicated one mode of binding. The present study further confirmed the groove binding mode of SBs with DNA.

4. Conclusion

A series of 8 new SBs were successfully synthesized from 2-(1-amino

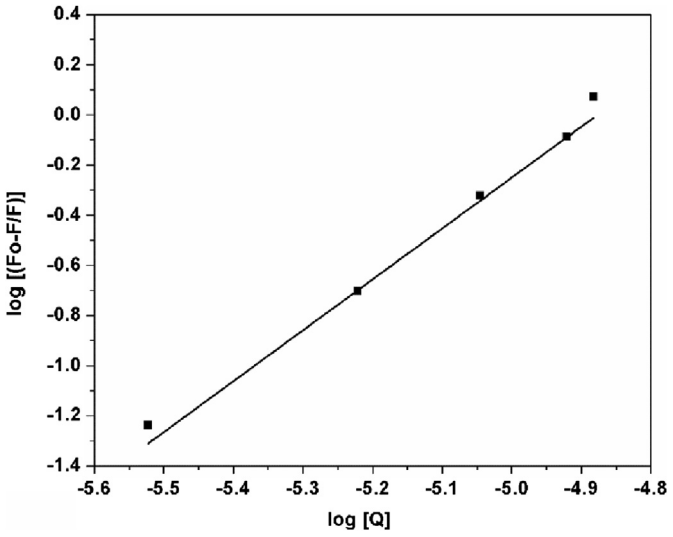

Fig. 9. The plot of log (Fo/F) vs log [Q] to determine value of association constant and number of binding sites of ct-DNA with SB **4d**.

Table 7
DNA binding constant (K), Stern-Volmer constant (Kq) and number of binding sites (n) for SBs **4a–4e** using plot of log [(Fo-F)/F] vs. log [Q].

Compound	K (M^{-1})	Kq (M^{-1})	N
4a	0.80×10^4	7.98×10^{12}	1.09
4b	1.05×10^4	8.43×10^{12}	1.03
4c	0.98×10^4	8.12×10^{12}	1.06
4d	1.12×10^4	8.78×10^{12}	1.02
4e	0.91×10^4	8.03×10^{12}	1.05
Thiabendazole	6.32×10^3	4.13×10^{11}	1.05
Olanzapine	2.28×10^3	2.13×10^{11}	1.01
Pregabain	2.24×10^3	1.59×10^{11}	1.04

benzyl) benzimidazole. The *in silico* screening predicted good pharmacokinetics and non-toxicity for the synthesized compounds. The DFT frontier orbital study determined global reactivity descriptors. The docking results supported non-covalent interactions into the groove binding mode. The interactions included H-bonding, pi-pi stacking, pi-anion and pi donor. The antimicrobial action showed enhanced inhibition for *E. coli* over *S. aureus* which further strengthens our statement that these SBs could be used for treating microbial infections caused by *E. coli*. The DNA binding study of SBs from heteroaryl carbonyl compounds, **4a–4e** was investigated using UV-Vis and fluorescence spectroscopy. The binding constant (K) was determined using absorption titration spectrofluoremetry and found to be in the range of 10^4. These studies confirmed that synthesized SBs act as minor groove binders with single mode of binding. Therefore, SBs have potential to act as new pharmacaphores for development of new antibiotic agents.

Declarations

Author contribution statement

Leena Khanna: Conceived and designed the experiments; Analyzed and interpreted the data; Contributed reagents, materials, analysis tools or data; Wrote the paper.

Sugandha Singhal: Performed the experiments; Analyzed and interpreted the data; Wrote the paper.

Pankaj Khanna: Conceived and designed the experiments; Analyzed and interpreted the data; Wrote the paper.

Funding statement

This work was supported by the Faculty Research Grant Scheme (FRGS), Guru Gobind Singh Indraprastha University, Dwarka, New Delhi.

Competing interest statement

The authors declare no conflict of interest.

Additional information

No additional information is available for this paper.

References

[1] T.H. Grossman, D.J. Bartels, S. Mullin, et al., Dual targeting of GyrB and ParE by a novel aminobenzimidazole class of antibacterial compounds, Antimicrob. Agents Chemother. 51 (2006) 657–666.
[2] N. Vashist, S.S. Sambi, B. Narasimhan, et al., Synthesis and biological profile of substituted benzimidazoles, Chem. Cent. J. 12 (2018) 125.
[3] T.J. Opperman, S.M. Kwasny, J.B. Li, et al., DNA targeting as a likely mechanism underlying the antibacterial activity of synthetic bis-indole antibiotics, Antimicrob. Agents Chemother. 60 (2016) 7067–7076.
[4] W.C. Tse, D.L. Boger, Sequence-selective DNA recognition: natural products and nature's lessons, Chem. Biol. 11 (2004) 1607–1617.
[5] S. Gupta, P. Pandya, G. Kumar, et al., Chemistry of Phytopotentials: Health, Energy and Environmental Perspectives, Springer, Berlin, Heidelberg ebook, 2012, pp. 149–153.
[6] A.A. Farahat, M.A. Ismail, A. Kumar, et al., Indole and benzimidazole bichalcophenes: synthesis, DNA binding and antiparasitic activity, Eur. J. Med. Chem. 143 (2018) 1590–1596.
[7] F. Jalali, P.S. Dorraji, Interaction of anthelmintic drug (thiabendazole) with DNA: spectroscopic and molecular modeling studies, Arab. J. Chem. 10 (2017) S3947–S3954.
[8] H. Wang, M. Jiang, F. Sun, et al., Screening, synthesis, and QSAR research on cinnamaldehyde-amino acid Schiff base compounds as antibacterial agents, Molecules 23 (2018) 3027.
[9] B. Iftikhar, K. Javed, M.S.U. Khan, et al., Synthesis, characterization and biological assay of Salicylaldehyde Schiff base Cu(II) complexes and their precursors, J. Mol. Struct. 1155 (2018) 337–348.
[10] M.M. Haque, M. Kudrat-E-Zahan, L.A. Banu, et al., Synthesis and characterization with antineoplastic, biochemical, cytotoxic, and antimicrobial studies of Schiff base Cu(II) ion complexes, Bioinorgan. Chem. Appl. (2015) 1–7.
[11] I.S. Ahmed, M.A. Kassem, Synthesis, solvatochromaticity and bioactivities of some transition metal complexes with 2-(R-benzylideneamino)-pyridin-3-ol Schiff base derivatives, Spectrochim. Acta A Mol. Biomol. Spectrosc. 77 (2010) 359–366.
[12] A.G.B. Dileepan, T.D. Prakash, A.G. Kumar, et al., Isatin based macrocyclic Schiff base ligands as novel candidates for antimicrobial and antioxidant drug design: In vitro DNA binding and biological studies, J. Photochem. Photobiol., B 183 (2018) 191–200.
[13] K.H.M.E. Tehrani, M. Hashemi, M. Hassan, et al., Synthesis and antibacterial activity of Schiff bases of 5-substituted isatins, Chin. Chem. Lett. 27 (2016) 221–225.
[14] L. Touafri, A. Hellal, S. Chafaa, et al., Synthesis, characterisation and DFT studies of three Schiff bases derived from histamine, J. Mol. Struct. 1149 (2017) 750–760.
[15] R. Sakhuja, S.S. Panda, L. Khanna, et al., Design and synthesis of spiro[indole-thiazolidine]spiro[indole-pyrans] as antimicrobial agents, Bioorg. Med. Chem. Lett 21 (2011) 5465–5469.
[16] P. Khanna, A. Saxena, L. Khanna, et al., Synthesis of novel symmetrical and unsymmetrical bis-spiro[indole-indazolyl-thiazolidine]-2,4′-diones, Arkivoc vii (2009) 119–125.
[17] M. Jain, R. Sakhuja, P. Khanna, et al., A facile synthesis of novel unsymmetrical bis-spiro[indole-pyrazolinyl-thiazolidine]-2,4'-diones, Arkivoc xv (2008) 54–64.
[18] M. Shaharyar, A. Mazumder, Salahuddin, et al., Synthesis, characterization and pharmacological screening of novel benzimidazole derivatives, Arab. J. Chem. 9 (2016) S342–S347.
[19] L. Khanna, S.S. Panda, P. Khanna, Synthetic routes to symmetric bisbenzimidazoles: a review, Mini-Reviews Org. Chem. 9 (2012) 381–396.
[20] R.K. Arora, N. Kaur, Y. Bansaln, et al., Novel coumarin–benzimidazole derivatives as antioxidants and safer anti-inflammatory agents, Acta Pharm. Sin. B 4 (2014) 368–375.
[21] F.A. Alasmary, A.M. Snelling, M.E. Alafeefy, et al., Synthesis and evaluation of selected benzimidazole derivatives as potential antimicrobial agents, Molecules 20 (2015) 15206–15223.
[22] N.S. El-Gohary, M.I. Shaaban, Synthesis and biological evaluation of a new series of benzimidazole derivatives as antimicrobial, antiquorum-sensing and antitumor agents, Eur. J. Med. Chem. 131 (2017) 255–262.
[23] Y. Luo, J.P. Yao, L. Yang, et al., Synthesis and anti-hepatitis B virus activity of a novel class of thiazolylbenzimidazole derivatives, Arch. Pharm. Chem. Life Sci. 344 (2011) 78–83.

[24] R.V. Shingalapur, K.M. Hosamani, R.S. Keri, Synthesis and evaluation of in vitro anti-microbial and anti-tubercular activity of 2-styryl benzimidazoles, Eur. J. Med. Chem. 44 (2009) 4244–4248.
[25] A. Lee-Dutra, K.L. Arienti, D.J. Buzard, et al., Identification of 2-arylbenzimidazoles as potent human histamine H4 receptor ligands, Bioorg. Med. Chem. Lett 16 (2006) 6043–6048.
[26] S. Oh, S. Kim, S. Kong, et al., Synthesis and biological evaluation of 2,3-dihydroimidazo[1,2-a]benzimidazole derivatives against Leishmania donovani and Trypanosoma cruzi, Eur. J. Med. Chem. 84 (2014) 395–403.
[27] S. Sogame, Y. Suenaga, M. Atobe, et al., Discovery of a benzimidazole series of ADAMTS-5 (aggrecanase-2) inhibitors by scaffold hopping, Eur. J. Med. Chem. 71 (2014) 250–258.
[28] B.A. Reddy, Synthesis, characterization and biological evaluation of 1, 2-disubstituted Benzimidazole derivatives using Mannich bases, Eur. J. Chem. 7 (2010) 222–226.
[29] N. Ranjan, S. Story, G. Fulcrand, et al., Selective inhibition of Escherichia coli RNA and DNA topoisomerase I by Hoechst 33258 derived mono- and bisbenzimidazoles, J. Med. Chem. 60 (2017) 4904–4922.
[30] A.S. Abu-Khadra, A.S. Afify, A. Mohamed, et al., Preparation, characterization and antimicrobial activity of Schiff base of (E) - N - (4-(thiophen-2-ylmethyleneamino) phenylsulfonyl) acetamide metal complexes, Open Bioact. Compd. J. 6 (2018) 1–10.
[31] A.A. Al-Amiery, Y.K. Al-Majedy, H.H. Ibrahim, et al., Antioxidant, antimicrobial, and theoretical studies of the thiosemicarbazone derivative Schiff base 2-(2-imino-1-methylimidazolidin-4-ylidene)hydrazinecarbothioamide (IMHC), Org. Med. Chem. Lett. 2 (2012) 4.
[32] N.K. Chaudhary, P. Mishra, Metal complexes of a novel Schiff base based on penicillin: characterization, molecular modeling, and antibacterial activity study, Bioinorgan. Chem. Appl. (2017) 1–13.
[33] K. Sudeepaa, N. Narsimhab, B. Aparnab, et al., Synthesis, spectral characterization, antimicrobial, DNA interactions and molecular modeling studies of metal complexes of 1, 3-benzothiazole carbohydrazone, J. Chem. Sci. 130 (2018) 52.
[34] R.R. Nasab, F. Hassanzadeh, M. Mansourian, Synthesis, antimicrobial evaluation and docking studies of some novel quinazolinone Schiff base derivatives, Res Pharma Sci 13 (2018) 213–221.
[35] S. Neidle, DNA minor-groove recognition by small molecules, Nat. Prod. Rep. 18 (2001) 291–309.
[36] A. Dadgarnezhad, I. Sheikhshoaie, F. Baghaei, Corrosion inhibitory effects of a new synthetic symmetrical Schiff-base on carbon steel in acid media, Anti-Corros Method M. 51 (2004) 266–271.
[37] M.H. Helal, Z.A. Al-Mudaris, M.H. Al-Douh, et al., Diaminobenzene schiff base, a novel class of DNA minor groove binder, Int. J. Oncol. 41 (2012) 504–510.
[38] S. Pasricha, D. Sharma, H. Ojha, et al., Luminescence, circular dichroism and in silico studies of binding interaction of synthesized naphthylchalcone derivatives with bovine serum albumin, Luminescence 32 (2017) 1252–1262.
[39] S.U. Rehman, Z. Yaseen, M.A. Husain, et al., Interaction of 6 mercaptopurine with calf thymus DNA – deciphering the binding mode and photoinduced DNA damage, PLoS One 9 (2017), e93913.
[40] M.A. Husain, H.M. Ishqi, S.U. Rehman, et al., Elucidating the interaction of sulindac with calf thymus DNA: biophysical and in silico molecular modelling approach, New J. Chem. 41 (2017) 14924–14935.
[41] N.M. Hosny, M.A. Husein, F.M. Radwan, et al., Synthesis, spectral, thermal and optical properties of Schiff-base complexes derived from 2(E)-2-((z)-4-hydroxypent-3-en-2-ylideneamino)-5-guanidinopentanoic acid and acetylacetone, J. Mol. Struct. 1143 (2017) 176–183.
[42] N. Shahabadi, S. Bagheri, Spectroscopic and molecular docking studies on the interaction of the drug olanzapine with calf thymus DNA, Spectrochim. Acta A Mol. Biomol. Spectrosc. 136 (2015) 1454–1459.
[43] N. Shahabadi, S. Amiri, Spectroscopic and computational studies on the interaction of DNA with pregabalin drug, Spectrochim. Acta A Mol. Biomol. Spectrosc. 138 (2015) 840–845.